PCCP

Cite this: *Phys. Chem. Chem. Phys.*, 2012, **14**, 2450–2454

www.rsc.org/pccp

PAPER

Investigation of band offsets of interface BiOCl:Bi_2WO_6: a first-principles study

Weichao Wang,[ab] Wenjuan Yang,[ab] Rong Chen,[cd] Xianbao Duan,[ab] Yunlong Tian,[ab] Dawen Zeng*[ab] and Bin Shan*[abe]

Received 9th October 2011, Accepted 7th December 2011
DOI: 10.1039/c2cp23186g

Density functional theory calculations are performed to study the band offsets at the interface of two photocatalytic materials BiOCl:Bi_2WO_6. It is found that the W–O bonded interface shows the most stability. An intrinsic interface fails to enhance the charge-carrier separation due to the improper band alignment between these two materials. Sulfur (S) is proposed to replace the bulk oxygen (O) site and thus tune the band edges of BiOCl to enhance the photocatalytic performance of the heterojunction. Furthermore, the presence of S provides an extra charge to generate a clean interface with minimal gap states that also benefits carrier migration across the heterojunction.

Photocatalysts have drawn great attention in both industrial and scientific communities due to their potential applications in energy and environmental related fields, such as hydrogen production[1] and water purification.[2–4] With incident photons' energies being larger than the band gap of a photocatalyst, electrons are excited to the conduction bands, resulting in the generation of electron–hole pairs. These photo-generated electrons and holes can react with H_2O and cause the evolution of H_2 and O_2 *via* water splitting reaction. Furthermore, electron transfers to O_2 and from H_2O can form highly reactive superoxide anions (O_2^-) and hydroxyl radicals ($^{\bullet}OH$) that are responsible for the decomposition of various organic contaminants. In both cases, alignments between water's and the phtocatalyst's molecular levels, light absorption capability, and electron–hole recombination rates play an essential role in determining the photocatalytic activity. To minimize electron–hole recombination rates and boost photocatalytic performance, people have attempted different approaches to enhance the carrier separation efficiency, such as the surface decoration of metal nanoparticles as electron traps[5] and the creation of heterojunctions by interfacing two well known catalysts.[6–11] In recent years, heterojunctions have received great attention in photocatalytic research. For instance, many heterojunctions such as WO_3/TiO_2,[6,7] MoO_3/TiO_2,[8] ZrO_2/TiO_2,[9] Fe_2O_3/TiO_2[10] and $BiOCl/Bi_2O_3$[11] have been fabricated and shown to provide different levels of performance boost, with many more other hetero-pairs still being under investigation. Nonetheless, formation of a heterojunction would improve the catalytic performance only if the band offsets (BOs) at the interface facilitate charge carrier separation, and this condition cannot always be guaranteed. In this article, a heterojunction consisting of Bi_2WO_6 and BiOCl is investigated since both components are popular candidates for the photocatalysis.[12,13] A first-principles method is used to investigate the interface BOs and thus disclose the interface impact on the overall catalytic performance. Some previous studies have utilized sulfur in engineering the band gap of a photocatlyst.[14,15] Through our theoretical study, further insights are provided to fine tune the BOs *via* sulfur (S) doping to enhance charge-carrier separation at the heterojunction.

Our calculations are based on the density functional theory (DFT) with the Perdew–Burke–Ernzerhof[16] version of the generalized gradient approximation (GGA-PBE) for the exchange–correlation potential, as implemented in a plane-wave basis code VASP.[17,18] The pseudopotential is described by the projector-augmented-wave (PAW) method.[19] An energy cutoff of 400 eV and an 8 × 8 × 1 k-point with a Γ centered k mesh were used in our calculations. The force on each atom was converged to 0.02 eV $Å^{-1}$ during the atomic structure optimization. For the supercells of our interface models, the atomic positions are relaxed and the interface distance re-optimized with a conjugate gradient (CG)[20] method.

[a] *State Key Laboratory of Material Processing and Die and Mould Technology, Huazhong University of Science and Technology, Wuhan 430074, Hubei, People's Republic of China. E-mail: bshan@mail.hust.edu.cn, dwzeng@mail.hust.edu.cn*
[b] *School of Materials Science and Engineering, Huazhong University of Science and Technology, Wuhan 430074, Hubei, People's Republic of China*
[c] *State Key Laboratory of Digital Manufacturing Equipment and Technology, Huazhong University of Science and Technology, Wuhan 430074, Hubei, People's Republic of China*
[d] *School of Mechanical Science and Engineering, Huazhong University of Science and Technology, Wuhan 430074, Hubei, People's Republic of China*
[e] *Department of Materials Science and Engineering, The University of Texas at Dallas, Richardson, TX 75080, USA*

We consider a model interface between an orthogonal BiOCl (CF12) and an orthogonal Bi_2WO_6 (*Pca*21). The unit cell of BiOCl is derived from the fluorite (CaF_2) structure [ref. 12]. It is a known tetragonal structure with lattice constants $a = b = 3.890$ Å and $c = 7.890$ Å. For Bi_2WO_6, the lattice constants are $a = 5.437$ Å, $b = 16.433$ Å, $c = 5.4587$ Å [ref. 21]. To accommodate the lattice constant difference, the (010)-oriented Bi_2WO_6 surface is stretched by ~1.0% and BiOCl is rotated counter-clockwise by 45° to match each other's surface (see Fig. 1a). At the interface, it could form either Bi–O, Bi–Cl or W–O bonds. Due to the stronger dissociation energy of W–O bonds (7.20 eV[22]) than Bi–O (3.37 eV[22]) and Bi–Cl (3.00 eV[22]), an interface model with W–O bonding is energetically more favorable. In order to systematically study the impacts of various interfacial bonding configurations on the BOs, Bi–O bonding interfaces with varying interfacial oxygen content are also considered. A 10 Å vacuum region is used to prevent the interactions between top and bottom atoms in the periodic slab images. Half the amount of oxygen atoms are removed from top and bottom surfaces to mimic Bi–O bulk bonds and thus electronically passivate both surfaces. We carefully tested different passivation schemes and the passivations of the top (Bi_2WO_6) and bottom (BiOCl) surfaces by removing oxygen atoms are shown to be most effective. Such passivation ensures that surface states are removed from top and bottom surfaces and all the calculated electronic states of interest originate from the interface. The whole slab is 40.26 Å thick with 80 atoms. The BiOCl slab consists of 4 layers of Bi, 4 layers of Cl and 3 layers of O, while the Bi_2WO_6 slab has 6 layers of Bi, 3 layers of W and 13 layers of O.

Fig. 1b shows the interface configuration with irrelevant atoms removed for clarity in visualization. The W–O bond length at the interface is 1.912 Å which is slightly smaller than that of the W–O bond in bulk Bi_2WO_6. Parts of interfacial oxygen atoms are removed from the interface to check the variation of the interface stability with respect to oxygen content. It is found that the O fully-terminated (four O atoms) interface shows the most stability for both Bi–O and W–O bonded interfaces. As a result, we focus on these two most stable interfaces for electronic analysis in this study. In order to compare the stabilities of Bi–O and W–O bonded interfaces, interface formation energies are calculated that are defined as the energy difference between the total system and individual components (BiOCl and Bi_2WO_6). To calculate the individual component energy of BiOCl, Bi_2WO_6 are removed from the interface; similarly, Bi_2WO_6 energy is calculated with BiOCl removed from the interface. The interface formation energy is then obtained by subtracting the individual component's energy from the total system energy. Compared with Bi–O bonded interface, the W–O-bonded interface is 1.66 eV $Å^{-2}$ more stable. Resulting from the strong W–O bond and the small planar strain (~1%), the corresponding interface (Fig. 1b) model is a realistic reflection of interfacial bonding situations and is adopted in all subsequent BO calculations, unless otherwise noted. Our charge difference plot also indicates that interfacial charge transfer takes place within a few atomic layers from the interface (~13 Å on the Bi_2WO_6 side and ~7 Å on the BiOCl side). Fig. 1c displays the

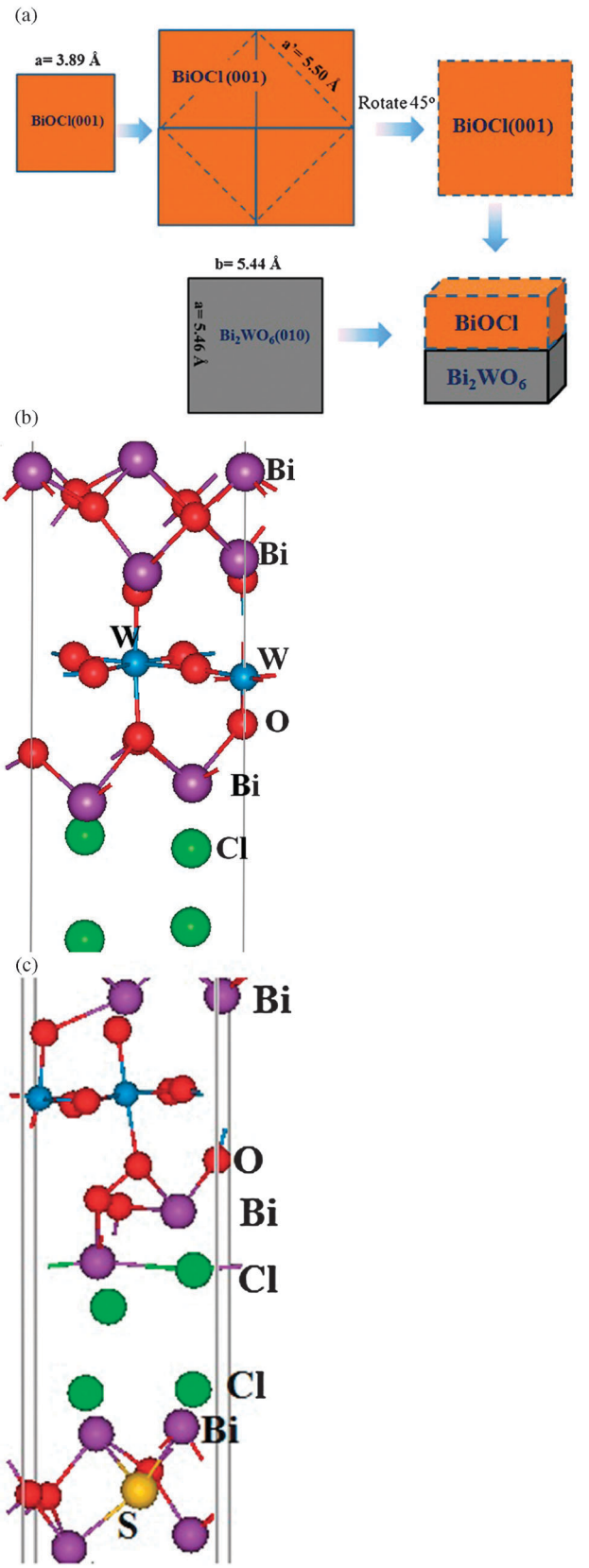

Fig. 1 (a) Schematic construction of the interface between BiOCl and Bi_2WO_6. Side views of the interface without (b) and with (c) S replacement of O sites in the BiOCl side. Green, pink, red, bright blue colors are Cl, Bi, O, and W atoms, respectively.

interface with one O site replaced by a sulfur atom in the bulk region of the BiOCl. Considering the atomic radius difference between O (48 pm) and S (88 pm),[23] a full structural relaxation including a unit cell volume change with the CG method [ref. 18] is performed here. After the structure optimization, *xy*-plane lattice length increases 0.04 Å comparing to that of an ideal interface. S bonds to three Bi atoms with an average bond length of 2.59 Å compared to the experimental value of 2.54 Å.[24] Compared an ideal interface, a 0.6% strain is introduced into the system. It is possible that doping of S could potentially influence the thermal stabilities of the interfaces. However, with regard to the only slightly bonding energy difference between Bi–O (3.37 eV [ref. 22]) and Bi–S (3.15 eV [ref. 22]), S-doping is not expected to significantly alter the structural stability. In fact, based on our calculations, the interface formation energy changes only slightly by around 0.05 eV $Å^{-2}$ when S dopes the interface.

The BO between BiOCl and Bi_2WO_6 is a key quantity in determining electron–hole separation and photocatalytic performance. In our study, BO is determined by the local density of states (LDOS) scheme.[25,26] Another method for calculating BO, namely the reference method,[27] is also performed to double check the accuracy of the BO and yields essentially the same result. To be consistent, we adopt the LDOS method throughout the present work. For a general slab model with asymmetric top and bottom surfaces, the vacuum level might not be flat due to the difference of the surface dipole moments. Here, top and bottom surfaces share the same amount of the oxygen atoms, specifically two, and thus dipole correction is negligible in the present calculation. We calculate the LDOS of atoms in the BiOCl and Bi_2WO_6 far away from the interface and extract the energy difference between their valence band maximums (VBMs). Due to the inaccuracy involved in the GGA in predicting the bandgap, the conduction band minimum (CBM) offsets are derived from the experimental values for the band gaps of BiOCl and Bi_2WO_6 (BiOCl: 3.46 eV;[28] Bi_2WO_6: 2.75 eV[29]). It is worth noting that the BOs between BiOCl and Bi_2WO_6 depend on detailed atomic geometries and charge transfers across the interface, in particular on interfacial oxygen terminations.[30,31] Similar phenomenon, *i.e.*, deviation of band alignment from the "Schottky-Mott" model, has also been observed in other metal/semiconductor, metal/organic, and semiconductor/semiconductor interfaces.[32–34]

In Fig. 2a, LDOSs of Bi_2WO_6 and BiOCl in the bulk region (far from interface) show that the VBM of Bi_2WO_6 leads by 0.46 eV. As it is well known that DFT is limited to produce right band gaps and describe the excited states,[35] we take the practical approach of calculating CB offsets utilizing the VB offsets and the experimental band gaps of individual materials. Using this approach, the deduced CBM offset is 0.25 eV. As a result, the band edges of Bi_2WO_6 nest into the band gap region of BiOCl, as schematically shown in Fig. 3(a). In photocatalysis, such band alignment is not beneficial for the separation of electron–hole pairs. As the incident light sheds on the BiOCl, electrons are excited to the conduction band and subsequently transferred to the CBM of Bi_2WO_6. Meanwhile, the created holes transfer to Bi_2WO_6 as well due to the lower

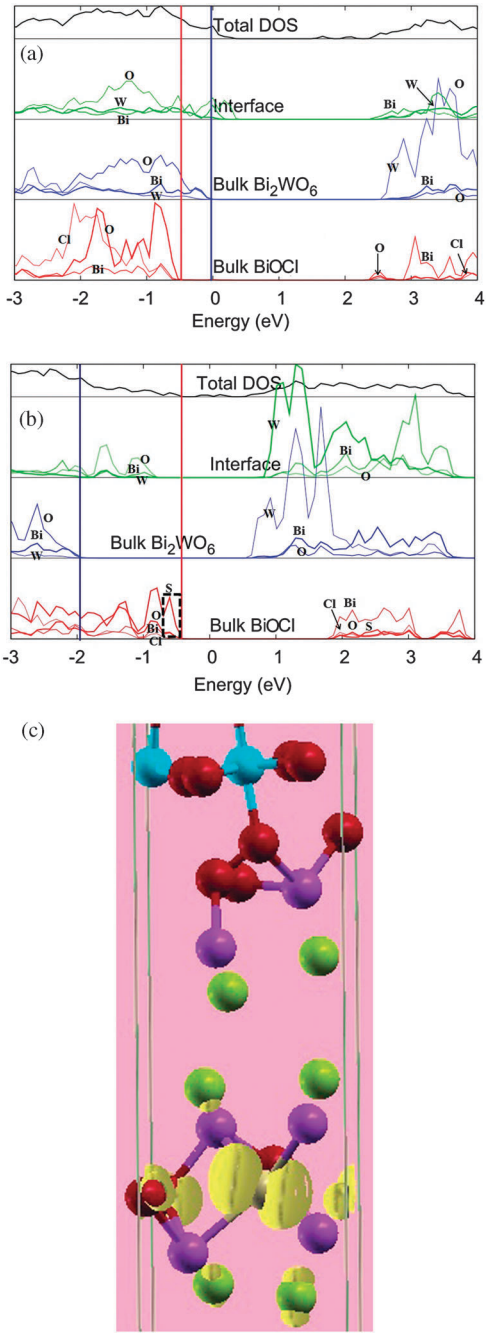

Fig. 2 Local density of states of bulk BiOCl, Bi_2WO_6 and interfacial atoms in the intrinsic interface (a) and the S-doped interface (b). Total density of states are normalized. (c) The partial charge distribution within the energy range of 0.2 eV marked with a dash box in (b). The charge density is 0.01 electron $Å^{-3}$. Blue and red lines indicate the VBM of Bi_2WO_6 and BiOCl on the two sides, respectively. The partial charge is in yellow color.

VBM of BiOCl (see Fig. 3(a)). Consequently, carriers do not separate at the heterojunction and recombination readily happens on the Bi_2WO_6 side. Moreover, slightly above the VBM of Bi_2WO_6, the existence of interfacial gap states (see Fig. 2a) might act as recombination centers and further degrade photocatalytic activities. To act as an ideal charge-carrier separator, the VBM

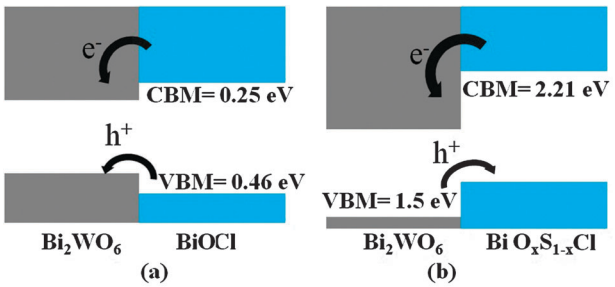

Fig. 3 Schematics of BOs of the W–O bonded (a) interface and (b) S-doped interface with great catalytic performance.

offset of these two materials should be flipped to facilitate charge carrier separation.

To better engineer the BO of this specific interface, it is insightful to further investigate the interface electronic structure. For both BiOCl and Bi_2WO_6 bulk materials, the VBMs are dominated by O p-orbitals. In bulk Bi_2WO_6 with a band gap of 2.50 eV, conduction band minimum is mainly dominated by W 5d orbitals which is consistent with previous work [ref. 13]. For bulk BiOCl, valence band maximum is mainly composed of Cl p and O p orbitals while Bi 6p orbitals dominate the CBM region [ref. 12]. To achieve the right VB offset, the leading edge locations of O p-orbitals must change accordingly. One possible solution to push up the BiOCl VBM is to increase the O p-orbital energy. From the theoretical point of view, introducing S to replace O sites could increase the VBM of BiOCl (S) due to the fact that S has the same valence state as O, while providing smaller ionization energy ($\sim$3.2 eV difference) [ref. 22]. From our simulation results, S-doped interface calculation (Fig. 2b) indeed provides the strong theoretical evidence, *i.e.*, the VB edge of BiOCl leads by 1.5 eV of Bi_2WO_6. From this analysis, we could obtain a general picture of tuning the band edge alignments at the interface. In fact, the VBOs are controlled by the highest occupied orbitals (O p-orbital) in the bulk region of the interface. Consequently, modifying this specific orbital energy results in an effective tuning of the band offsets. To further confirm the role of S, we plot the partial charge distribution (see Fig. 2c) within the energy range of $\pm$0.2 eV in the valence bands of BiOCl, as marked with a dash box in Fig. 2b. It is clearly shown that the partial charge distributes around the S atom with a π-like behavior.

Besides band offset issues, large amounts of interfacial states might also act as carrier traps and degrade heterojunction performance. From Fig. 2a, certain states within the band gap region arise from the planar strain at the interface and could be removed by replacing the right amount of O at the interface by materials with less electro-negativity than O, such as S. In the case of the S-doped interface, it shows a clean band gap based on local density of states analysis (Fig. 2b), which confirms the superiority of S in facilitating charge carrier separation. Based on the same argument, Se might play the same role attributed to the almost same electronegativity between S (2.5) and Se (2.6). However, Se might cause the stability issue arising from the lesser bond strength of Se–Bi (2.80 eV) than S–Bi (3.15 eV) [ref. 22].

In conclusion, the first-principles method has been used to study the band offsets of the BiOCl:Bi_2WO_6 interface. We find that the intrinsic stable interface fails to provide advantages of carrier separation due to improper band alignments. This can be overcome by the incorporation of S into O sites in the BiOCl bulk to reverse the valence band offsets and enhance photocatalytic performance.

Acknowledgements

This work is supported by the National Natural Science Foundation of China (11004068) and PCSIRT (Program for Changjiang Scholars and Innovative Research Team in University) and Program for New Century Excellent Talents in University (NCET). D.W. Zeng would like to acknowledge the support from the National Basic Research Program of China (Grant No. 2009CB939705 and 2009CB939702). The authors acknowledge the Texas Advanced Computing Center (TACC) at The University of Texas at Austin (http://www.tacc.utexas.edu) and the High Performance Computing Center experimental testbed in SCTS/CGCL (http://grid.hust.edu.cn/hpcc) for providing grid resources that have contributed to the research results reported within this paper.

References

1 A. Kudo and Y. Miseki, *Chem. Soc. Rev.*, 2009, **38**, 253.
2 Z. Zou, J. Ye, K. Sayama and H. Arakawa, *Nature*, 2001, **414**, 625.
3 K. Maeda, K. Teramura, D. Lu, T. Takata, N. Saito, Y. Inoue and K. Domen, *Nature*, 2006, **440**, 295.
4 C. Hsiao, C. Lee and D. Ollis, *J. Catal.*, 1983, **82**, 418.
5 J. Wu and C. H. Tseng, *Appl. Catal., B*, 2006, **66**, 51.
6 N. Serpone, P. Maruthamuthu, P. Pichat, E. Pelizzetti and H. Hidaka, *J. Photochem. Photobiol., A*, 1995, **85**, 247.
7 I. Shiyanovskaya and M. Hepel, *J. Electrochem. Soc.*, 1998, **145**, 3981.
8 J. Papp, S. Soled, K. Dwight and A. Wold, *Chem. Mater.*, 1994, **6**, 496.
9 J. Yu, J. Lin and R. Kwok, *J. Phys. Chem. B*, 1998, **102**, 5094.
10 M. Sadeghi, W. Liu, T. Zhang, P. Stavropoulos and B. Levy, *J. Phys. Chem.*, 1996, **100**, 19466.
11 Y. Li, J. Wang, H. Yao, L. Dang and Z. Li, *Catal. Commun.*, 2011, **10**, 660.
12 K. Zhang, C. Liu, F. Huang, C. Zheng and W. Wang, *Appl. Catal., B*, 2006, **68**, 125.
13 H. Fu, L. Zhang, W. Yao and Y. Zhu, *Appl. Catal., B*, 2006, **66**, 100.
14 T. Umebayashi, T. Yamaki, H. Itoh and K. Asai, *Appl. Phys. Lett.*, 2002, **81**, 454.
15 N. Umezawa, A. Janotti, P. Rinke, T. Chikyow and C. G. Van de Walle, *Appl. Phys. Lett.*, 2008, **92**, 041104.
16 J. Perdew, K. Burke and M. Ernzerhof, *Phys. Rev. Lett.*, 1996, **77**, 3865.
17 G. Kresse and J. Furthmüller, *Comput. Mater. Sci.*, 1996, **6**, 15.
18 G. Kresse and J. Furthmüller, *Phys. Rev. B*, 1996, **54**, 8245.
19 P. E. Blochl, *Phys. Rev. B*, 1994, **50**, 17953.
20 W. Press, B. Flannery, S. Teukolsky and W. Vetterling, *Numerical Recipes*, Cambridge University Press, New York, 1986.
21 M. S. Islam, S. Lazure, R. Vannier, G. Nowogrocki and G. Mairesse, *J. Mater. Chem.*, 1998, **8**(3), 655–660.
22 CRC Handbook of Chemistry and Physics, 90th Edition.
23 http://www.webelements.com/.
24 R. Long and N. English, *J. Phys. Chem. C*, 2009, **113**(19), 8373.
25 J. Bass, M. Oloumi and C. Matthai, *J. Phys.: Condens Matter*, 1989, **1**, 10625.

26 J. Robertson and P. W. Peacock, *Phys. Status Solidi B*, 2004, **241**, 2236.
27 A. Janotti and C. G. Van de Walle, *Phys. Rev. B*, 2007, **75**, 121201.
28 K. Zhang, C. liu, F. Huang, C. Zheng and W. Wang, *Appl. Catal., B*, 2006, **68**, 125.
29 Y. Li, J. Liu and X. Huang, *Nanoscale Res. Lett.*, 2008, **3**, 365.
30 W. Wang, K. Xiong, R. M. Wallace and K. Cho, *Appl. Surf. Sci*, 2010, **256**, 6569.
31 W. Wang, K. Xiong, R. M. Wallace and K. Cho, *J. Phys. Chem. C*, 2010, **114**, 22610.
32 B. Shan and K. Cho, *Phys. Rev. B*, 2004, **70**, 233405.
33 I. G. Hill, A. Rajagopal, A. Kahn and Y. Hu, *Appl. Phys. Lett.*, 1998, **73**, 662.
34 C. Gong, G. Lee, B. Shan, E. M. Vogel, R. M. Wallace and K. Cho, *J. Appl. Phys.*, 2010, **108**, 123711.
35 W. Kohn, *Rev. Mod. Phys.*, 1999, **71**, 1253.

